J. Fluid Mech. (2004), *vol.* 502, *pp.* 207–232.
DOI: 10.1017/S0022112003007547 Printed in the United Kingdom

Stability of vortices in a two-layer ocean with uniform potential vorticity in the lower layer

By E. S. BENILOV

Department of Mathematics, University of Limerick, Ireland

(Received 17 March 2003 and in revised form 21 July 2003)

It is well-known that oceanic vortices exist for years, whereas almost all theoretical studies indicate that they must be unstable. A rare exception is the work by Dewar & Killworth (1995), who demonstrated that a Gaussian vortex in the upper layer of a two-layer ocean becomes stable if accompanied by a weak co-rotating circulation in the lower layer. Note that this paper assumed the lower-layer circulation to have the same profile as the main (upper-layer) vortex. The present paper considers the case where the profile of the circulation in the lower layer is determined by the condition that potential vorticity (PV) there is constant – which models a vortex surrounded by water of a different origin. Given that most oceanic vortices are shed by frontal currents, such model appears to be more realistic than any *ad hoc* choice. The stability of vortices with uniform lower-layer PV is examined for both quasigeostrophic and ageostrophic cases, numerically and asymptotically, assuming that the upper layer of the ocean is thin. It is shown that such vortices are stable for a wide range of parameters. The effect of vortex stabilization is interpreted through representation of the unstable disturbance by two phase-locked Rossby waves, rotating around the vortex in the upper and lower layers. Then, if the lower-layer PV gradient is zero, it cannot support the corresponding wave, which inhibits the instability.

1. Introduction

The contradiction between experimental and theoretical estimates of the lifespan of oceanic vortices (rings) was identified more than two decades ago. Observations (e.g. Lai & Richardson 1977) suggest that rings exist for years, whereas theoretical studies (e.g. Ikeda 1981; Flierl 1988; Helfrich & Send 1988; Carton & McWilliams 1989; Ripa 1992; Killworth, Blundell & Dewar 1997; Benilov, Broutman & Kuznetsova 1997; Benilov 2003; Katsman *et al.* 2003) indicate that they are unstable. Only two theoretical papers claimed to have found examples of stable vortices.

The first such claim was made by Paldor & Nof (1990). Using the model of a two-layer ocean, they considered a solid-body rotating vortex in the upper layer, with no flow in the lower layer, and demonstrated that it is stable if sufficiently thin (less than, approximately, a quarter of the total depth of the ocean). This result would resolve the paradox, as most oceanic vortices are indeed thin. Later, however, Benilov (2003) examined thin vortices of arbitrary shape, and showed that their instability is caused by the so-called critical levels – which devalued the result of Paldor & Nof (1990): a solid-body vortex does not have critical levels and, therefore, it is not a good model for (differentially rotating) oceanic rings.

Another mechanism of ring stabilization has been put forward by Dewar & Killworth (1995), who considered a vortex in the upper layer and a relatively weak

co-rotating circulation in the lower layer ('deep flow'). It turned out that the latter can stabilize the vortex, or at least considerably reduce the growth rate of instability. This result was later extended to other vortex shapes by Katsman *et al.* (2003): in all examples considered, a co-rotating deep flow reduced the growth rate (although no profile other than the Gaussian one would become entirely stable).

Before we describe the results of the present paper, note that Dewar & Killworth (1995) and Katsman *et al.* (2003) assumed that the deep circulation has the same shape as the upper-layer vortex. We shall use a different approach: the profile of the deep flow will be derived from the assumption that potential vorticity (PV) in the lower layer is constant. Such a model is suggested by the fact that most oceanic vortices are shed by unstable frontal currents: when a vortex moves away from the current and arrives at a new location, the PV field below it cannot change and remains equal to its initial, background value. Observe also that the interface displacement, caused by the vortex, contributes to the lower-layer PV – hence, to maintain its initial value, the lower layer spins up. Remarkably, the resulting circulation is always *co*-, and never *counter*-, rotating.

The present paper builds on the foundation of Dewar & Killworth's (1995) physical idea, using the mathematical tool developed by Benilov (2003). We shall consider vortices in a two-layer ocean with thin upper layer and weak circulation in the lower layer. An asymptotic stability criterion, based on these two assumptions, will be developed. It will be demonstrated that this criterion is satisfied for the most interesting case of vortices with uniform PV in the lower layer, regardless of their profiles in the upper layer.

The paper has the following structure. In § 2, we shall describe the setting, formulate the governing (quasi-geostrophic) equations, and derive an eigenvalue problem for harmonic disturbances (normal modes). In § 3, through numerical solution of the eigenvalue problem, we shall present several examples of stable vortices with different profiles in the upper layer and uniform PV in the lower layer. In §§ 4–6, we shall derive an asymptotic stability criterion for thin vortices with a weak deep flow. In § 7, this criterion will be applied to vortices with constant lower-layer PV. In § 8, we shall extend the asymptotic results to ageostrophic vortices.

2. Governing equations

Consider a two-layer ocean with rigid lid and flat bottom, and let the densities and depths of the layers be $\rho_{1,2}$ and $H_{*1,2}$ (where subscript 1 denotes the upper layer). We shall also introduce the upper-layer deformation radius

$$L_d = \frac{1}{f}\sqrt{g' H_{*1}},$$

where $g' = g(\rho_2 - \rho_1)/\rho_2$ is the reduced acceleration due to gravity and f is the Coriolis parameter. Using L_d and the characteristic velocity V_{*1} of the flow in the upper layer, we shall introduce the following non-dimensional variables:

$$t = \frac{V_{*1} t_*}{L_d}, \qquad (x, y) = \frac{(x_*, y_*)}{L_d}, \qquad \psi_{1,2} = \frac{\psi_{*1,2}}{L_d V_{*1}},$$

where t is the time, (x, y) are the spatial coordinates, $\psi_{1,2}$ are the streamfunctions, and the asterisk denotes dimensional variables.

For the description of the vortices, we shall employ the standard quasi-geostrophic (QG) equations on the f-plane,

$$\frac{\partial}{\partial t}(\nabla^2\psi_1 - \psi_1 + \psi_2) + J(\psi_1, \nabla^2\psi_1 + \psi_2) = 0, \tag{2.1}$$

$$\frac{\partial}{\partial t}(\nabla^2\psi_2 - \varepsilon\psi_2 + \varepsilon\psi_1) + J(\psi_2, \nabla^2\psi_2 + \varepsilon\psi_1) = 0, \tag{2.2}$$

where $J(\psi_1, \psi_2)$ is the Jacobian operator and ε is the depth ratio,

$$\varepsilon = \frac{H_{*1}}{H_{*2}}.$$

We are concerned with the linear stability of radially symmetric vortices, and assume

$$\psi_{1,2} = \Psi_{1,2}(r) + \psi'_{1,2}(r, \theta, t), \tag{2.3}$$

where the $\Psi_{1,2}$ describe the vortex, $\psi_{1,2}$ describe the disturbance, and (r, θ) are polar coordinates. Then we linearize the governing equations against the background of the vortex solution, i.e. substitute (2.3) into (2.1)–(2.2) and omit the nonlinear terms,

$$\frac{\partial}{\partial t}(\nabla^2\psi'_1 - \psi'_1 + \psi'_2) + J(\Psi_1, \nabla^2\psi'_1 + \psi'_2) + J(\psi'_1, \nabla^2\Psi_1 + \Psi_2) = 0,$$

$$\frac{\partial}{\partial t}(\nabla^2\psi'_2 - \varepsilon\psi'_2 + \varepsilon\psi'_1) + J(\Psi_2, \nabla^2\psi'_1 + \varepsilon\psi'_1) + J(\psi'_2, \nabla^2\Psi_1 + \varepsilon\Psi_1) = 0.$$

In this paper, we are concerned with harmonic disturbances (normal modes),

$$\psi'_{1,2}(r, \theta, t) = \mathrm{Re}\left[\psi_{1,2}(r)\mathrm{e}^{\mathrm{i}k(\theta - ct)}\right],$$

where k and c are the azimuthal wavenumber and angular phase speed, respectively. Then, the governing equations yield

$$(cr - V_1)\left[\frac{1}{r}\frac{\mathrm{d}}{\mathrm{d}r}\left(r\frac{\mathrm{d}\psi_1}{\mathrm{d}r}\right) - \frac{k^2}{r^2}\psi_1 - \psi_1 + \psi_2\right] + Q'_1\psi_1 = 0, \tag{2.4}$$

$$(cr - V_2)\left[\frac{1}{r}\frac{\mathrm{d}}{\mathrm{d}r}\left(r\frac{\mathrm{d}\psi_2}{\mathrm{d}r}\right) - \frac{k^2}{r^2}\psi_2 - \varepsilon\psi_2 + \varepsilon\psi_1\right] + Q'_2\psi_2 = 0, \tag{2.5}$$

where

$$V_{1,2} = \frac{\mathrm{d}\Psi_{1,2}}{\mathrm{d}r}$$

are the swirl velocities in the layers and

$$Q'_1 = \frac{\mathrm{d}}{\mathrm{d}r}\left[\frac{1}{r}\frac{\mathrm{d}}{\mathrm{d}r}(rV_1)\right] - V_1 + V_2, \qquad Q'_2 = \frac{\mathrm{d}}{\mathrm{d}r}\left[\frac{1}{r}\frac{\mathrm{d}}{\mathrm{d}r}(rV_2)\right] - \varepsilon V_2 + \varepsilon V_1$$

are the corresponding PV gradients.

Equations (2.4)–(2.5) should be supplemented by the usual boundary conditions,

$$\psi_{1,2}(0) = \psi_{1,2}(\infty) = 0. \tag{2.6}$$

Equations (2.4)–(2.6) form an eigenvalue problem, where c is the eigenvalue. If $\mathrm{Im}\, c \neq 0$, the vortex is unstable. (Strictly speaking, instability requires $\mathrm{Im}\, c > 0$, but complex eigenvalues in problem (2.4)–(2.6) always come in complex-conjugate pairs.)

We shall assume that $V_1(r)$ and $V_2(r)$ are smooth functions, decaying as $r \to \infty$ and vanishing at $r = 0$ (the latter condition guarantees that the vortex is smooth at

its centre). We shall also assume that

$$0 < \int_0^\infty r^2 V_1 \, \mathrm{d}r < \infty, \tag{2.7}$$

i.e. the upper-layer net angular momentum of the vortex is finite and non-zero.

3. Numerical results

Now, problem (2.4)–(2.6) will be analysed numerically. In the first subsection, we shall briefly discuss compensated vortices, i.e. those that have no flow in the lower layer (this will be mostly an adaptation of Benilov's (2003) results for our present needs). Then we shall examine several examples of vortices with uniform PV in the lower layer.

3.1. *Compensated vortices*

In this case, the lower layer is at rest,

$$V_2 = 0, \tag{3.1}$$

and we consider the following three examples of flow in the upper layer:

$$V_{1G} = \frac{r}{r_0} \exp\left(-\frac{r^2}{2r_0^2}\right), \tag{3.2}$$

$$V_{1A} = \frac{r}{r_0}\left(1 + \frac{r^2}{5r_0^2}\right)^{-3}, \tag{3.3}$$

$$V_{1S} = \frac{r}{r_0}\mathrm{sech}\left(\frac{1.186\, r}{r_0}\right), \tag{3.4}$$

where r_0 is the non-dimensional radius of the vortex (i.e. the ratio of its dimensional radius to the deformation radius based on the upper-layer depth). The coefficients in these expressions have been chosen to ensure that the maximum of $V_1(r)$ is located at $r = r_0$ (for (3.4), this equality is approximate, $r \approx r_0$). Profiles (3.2)–(3.4) will be referred to as the Gaussian vortex, Algebraic vortex, and the Sech vortex, respectively. The corresponding profiles of the upper-layer angular velocity, V_1/r, are shown in figure 1(a) – to a naked eye, the three profiles are not very different.

The stability of vortices (3.2), (3.1); (3.3), (3.1); and (3.4), (3.1) was examined by Benilov (2003) for a wide range of parameters, both asymptotically and numerically (hereinafter, this work will be referred to as B03). It was demonstrated that the most unstable azimuthal wavenumber is either $k = 1$ or $k = 2$. It was also shown that, for a given k, the Gaussian vortex admits a finite number of eigenvalues, with the corresponding lower-layer eigenfunctions having a different number of nodes. The first eigenvalue always has the highest growth rate (here, the eigenvalues are enumerated according to the number of nodes of the lower-layer eigenfunction: the first eigenfunction has no nodes, the second one has one node, etc.). Moreover, when parameters of a stable Gaussian vortex change and make it unstable, the first mode becomes unstable before the others – which makes it a 'stability indicator'. The Sech vortex, in turn, may have either a finite or infinite number of eigenvalues (depending on whether $r_0 < 1.186$ or $r_0 > 1.186$), but the first mode is, again, the stability indicator. Finally, the Algebraic vortex admits infinitely many eigenvalues for each k, and the first eigenvalue loses stability after all the others – although, in many cases, it is still the most unstable one (when, of course, it is unstable).

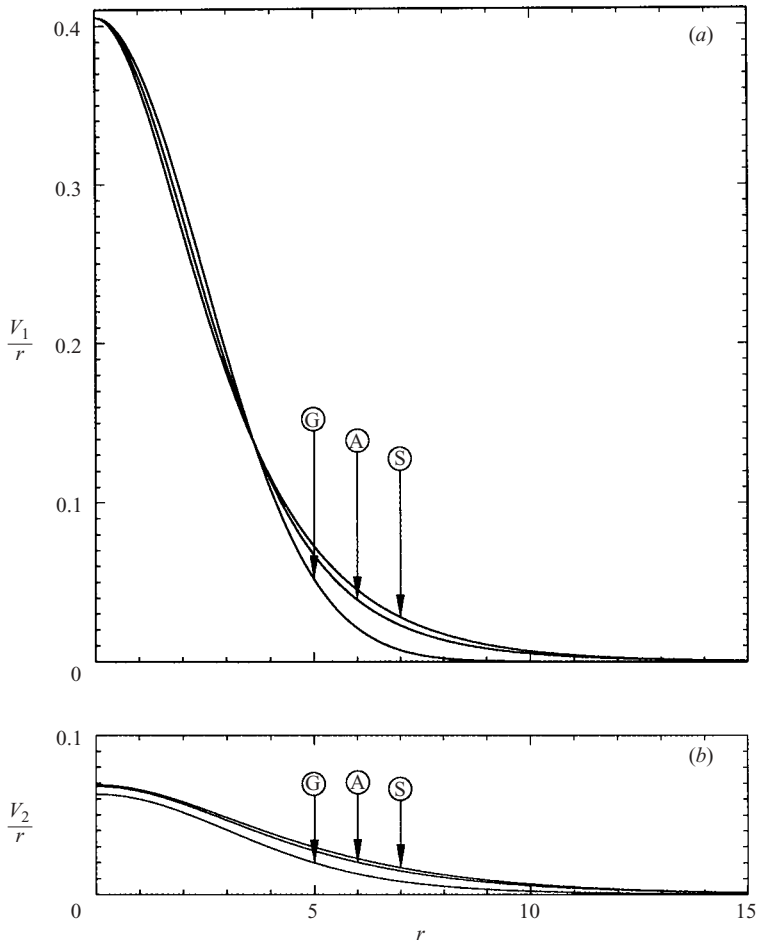

FIGURE 1. Angular velocity of vortex profiles considered in the paper. (*a*) In the upper layer, the vortex is determined by (3.2), or (3.3), or (3.4) (the Gaussian, or Algebraic, or Sech profiles, marked by G, A, and S, respectively). (*b*) In the lower layer, the profile of the vortex is determined by the condition that PV is constant (i.e. it satisfies (3.7)–(3.8)).

The most important characteristic of a vortex profile is the corresponding marginal stability curve on the (ε, r_0)-plane – we have computed it for compensated vortices (3.1), (3.2); (3.1), (3.3); (3.1), (3.4) for the first eigenvalue of the second azimuthal wavenumber, $k = 2$. As $\varepsilon \to 0$ (the limit of an infinitely thin upper layer), the solution of the eigenvalue problem (2.4)–(2.6) is increasingly difficult to compute, and we complement the numerical solution by an asymptotic one, obtained via a method developed in B03.

The results of these calculations are shown in figure 2.

Observe that the Gaussian profile has two regions of instability (see figure 2*a*). The narrow strip with small r_0 corresponds to *barotropic* instability, caused by strong *horizontal* shear; whereas vortices with large r_0 are unstable *baroclinically* due to *vertical* shear. Note that moderate horizontal shear is a stabilizing influence: for vortices with moderate values of r_0, it neutralizes the effect of vertical shear and makes them stable. Observe also that the Algebraic and Sech profiles are barotropically stable.

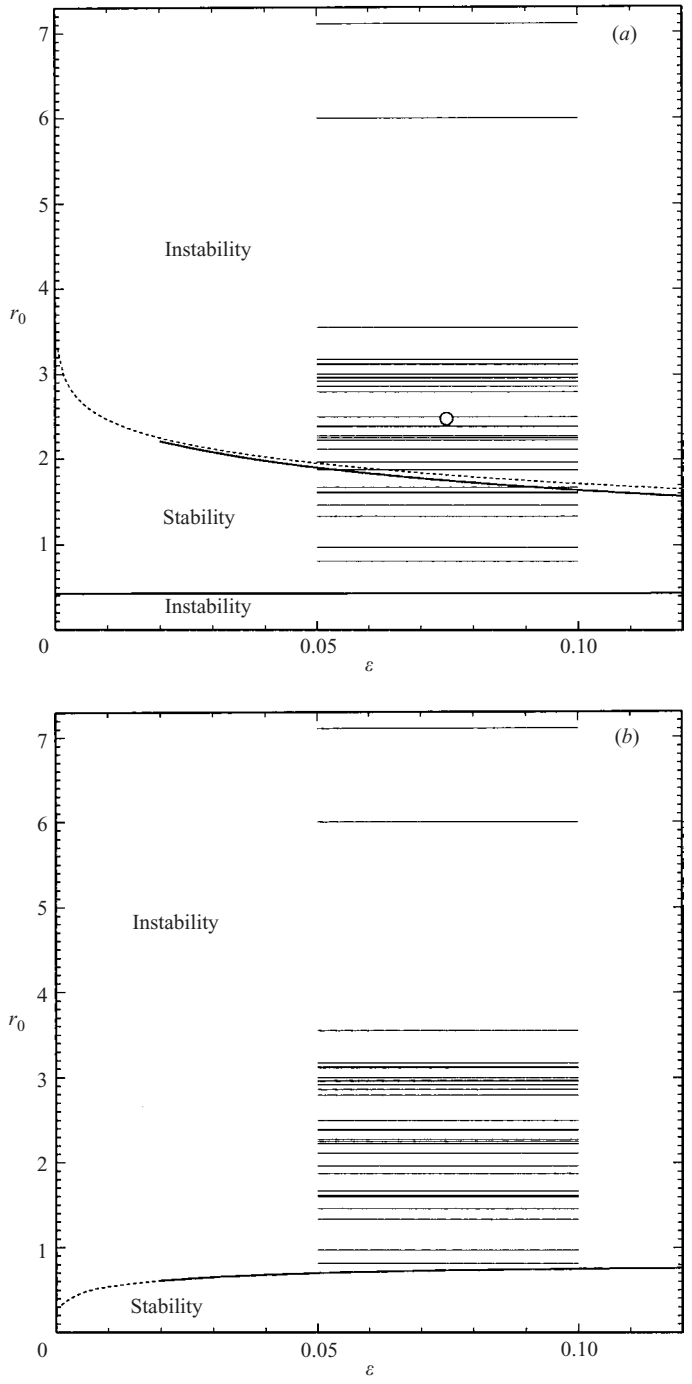

FIGURE 2. For legend see facing page.

To place the above results in an oceanographic context, figure 2 shows the parameters of the 35 rings catalogued by Olson (1991) (this paper will be referred to as O91). Unfortunately, O91 provides no data on the depth ratio ε, and we assumed,

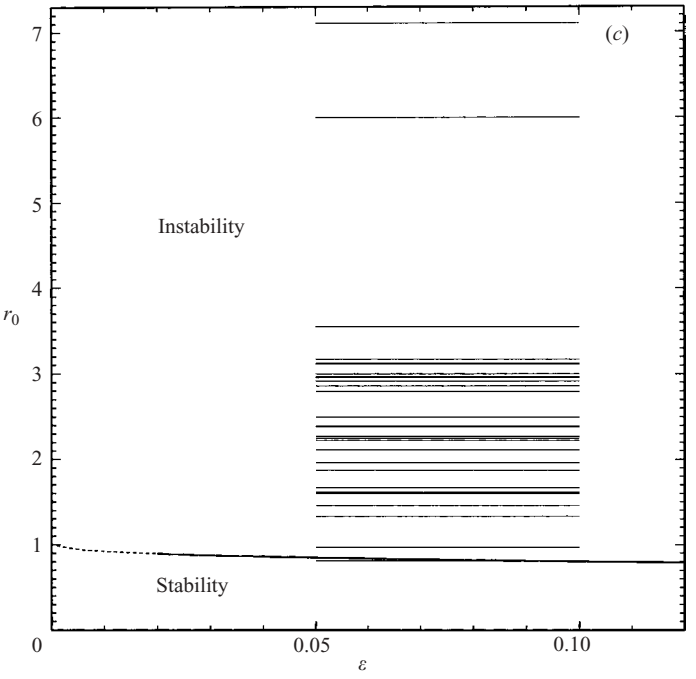

FIGURE 2. Stability of compensated vortices with respect to the first mode of $k = 2$, on the (ε, r_0)-plane (ε is the depth ratio of the ocean, r_0 is the non-dimensional radius of the vortex). Solid curve shows the numerical results, dotted curve shows the asymptotic results (based on $\varepsilon \ll 1$); horizontal segments show the parameters of rings catalogued by Olson (1991). (*a*) Gaussian vortex (3.2), (*b*) Algebraic vortex (3.3), (*c*) Sech vortex (3.4). The circle in the centre of (*a*) shows the 'mean' vortex (3.5)–(3.6).

on a more or less *ad hoc* basis, that

$$0.05 \lesssim \varepsilon \lesssim 0.1.$$

Thus, each ring in figure 2 is represented by an interval with a fixed r_0 , but uncertain ε. One can see that the Algebraic model (figure 2*b*) predicts that all rings are unstable for all possible ε, and the predictions of the Sech model are similar. The Gaussian model is the only one producing rings which are stable for the whole ε range (these are the six rings with the smallest values of r_0). Overall, the proportion of stable vortices is far too low to account for oceanic observations.

Still, one might argue that the instability is so weak that unstable rings survive for a long time before breaking up (which would explain the lifespans observed). To eliminate this possibility, we have computed the growth rate for the Gaussian vortex of radius 65 km (which is the average over the rings listed in O91) in the ocean with deformation radius of 27 km (which is, again, an average derived from O91). Non-dimensionally, these values correspond to

$$r_0 = 2.468, \tag{3.5}$$

and we assumed the mid-point of the ε range:

$$\varepsilon = 0.075 \tag{3.6}$$

(values (3.5)–(3.6) are shown in figure 2*a* by a circle). In this case, the first eigenvalue with $k = 2$ is the most unstable one, with a growth rate of $k \operatorname{Im} \omega \approx 0.01711$. To

put this into dimensional terms, we need to fix the ring's maximum swirl velocity. Unfortunately, O91 provides only the 'absolute' maximum of the swirl velocity, whereas we need the maximum of the swirl velocity averaged over the upper layer's depth, $V_{*1\,\max}$ (which is a restriction imposed by the two-layer model). Estimating $V_{*1\,\max}$ to be within the range of 0.1–0.25 m s^{-1}, we obtain the e-folding time range of 111–44 days, respectively. Clearly, this is much shorter than the lifespans of most oceanic rings.

Thus, the model of compensated vortices cannot explain the observed longevity of rings.

3.2. *Vortices with uniform PV in the lower layer*

For the upper-layer velocity, we considered the same three examples as before, (3.2)–(3.4). The lower-layer velocity, in turn, was assumed to satisfy the condition that the PV gradient is zero,

$$\frac{\mathrm{d}}{\mathrm{d}r}\left[\frac{1}{r}\frac{\mathrm{d}}{\mathrm{d}r}(rV_2)\right] - \varepsilon V_2 + \varepsilon V_1 = 0, \tag{3.7}$$

and the usual boundary conditions

$$V_2(0) = V_2(\infty) = 0. \tag{3.8}$$

As an illustration, figure 1(*b*) shows the solution of the boundary-value problem (3.7)–(3.8) for the Gaussian, Algebraic, and Sech vortices, with the 'mean' parameters (3.5)–(3.6).

It was found that vortices with an Algebraic or Sech profile in the upper layer, and uniform PV in the lower layer, are stable for all values of ε and r_0 – a thorough search has not yielded a single unstable vortex. For the Gaussian profile in the upper layer (and, again, uniform PV in the lower one), the region of barotropically unstable vortices looks almost the same as that for compensated vortices, but the region of baroclinically unstable vortices disappears completely. Thus, the model of uniform PV in the lower layer predicts that all rings listed in O91 are stable.

To illustrate the transition from compensated vortices to those with uniform PV in the lower layer, consider

$$V_2 = \alpha\,(V_2)_{uPV} \tag{3.9}$$

where $(V_2)_{uPV}$ is the solution of the uniform-PV problem (3.7)–(3.8), and α is a number between 0 (compensated vortex) and 1 (uniform PV in the lower layer). A large number of vortices, with various parameters, were tested for stability, and in all cases the growth rate vanished for some $\alpha < 1$. A typical behaviour of the non-dimensional growth rate is shown in figure 3 for the 'mean' vortex (3.5)–(3.6): one can see that, for all three upper-layer profiles, the vortex becomes stable at $\alpha \approx 0.65$. It is also worth observing that, for $0.45 \lesssim \alpha \lesssim 0.65$, the three curves virtually coincide.

We have also computed the marginal stability curves for $\alpha = 0.65$ (the numerical technique is described in Appendix A). For the Algebraic and Sech upper-layer profiles, these curves are very close, and we show only the one corresponding to the former (see figure 4*b*). The Gaussian profile is different (see figure 4*a*), but only as far as barotropic instability is concerned; the curve separating baroclinically unstable vortices from the stable ones is almost the same as that in the other two cases.

One can see that, for non-compensated vortices determined by (3.9) with $\alpha = 0.65$, the stability region has noticeably expanded (compare figures 4*a*, *b* to 2*a*, *b*). Moreover, the growth rate of vortices that are still unstable has fallen dramatically. Consider

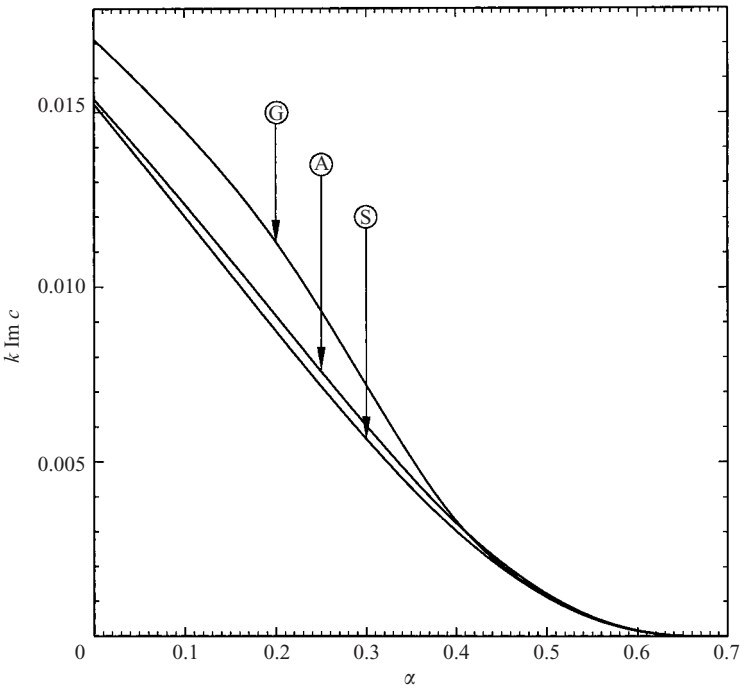

FIGURE 3. The growth rate of the first mode of $k = 2$, for the 'mean' vortex ($\varepsilon = 0.075$, $r_0 = 2.468$), *vs.* the amplitude α of the lower-layer circulation. The lower-layer velocity is determined by (3.9) (where $\alpha = 0$ corresponds to compensated vortices, and $\alpha = 1$ corresponds to vortices with uniform PV in the lower layer); G, A, and S mark the Gaussian, Algebraic, and Sech vortex profiles.

the three rings on the O91 list that have the largest values of r_0,

$$r_0 = 7.105, \quad 6.000, \quad 3.548 \tag{3.10}$$

(in figure 4*a*, these values are marked by circles with numbers 1–3, respectively). The corresponding values of the deformation radius, extracted from O91, are

$$L_d = 42, \ 10, \ 19\,\text{km}.$$

We shall assume that

$$\varepsilon = 0.1, \tag{3.11}$$

which is the most unstable value of the ε range considered before. Finally, we put

$$V_{*1\,\max} = 0.25\,\text{m}\,\text{s}^{-1},$$

which is, again, the most unstable value of the range considered. For rings with these parameters, with a Gaussian profile in the upper layer and profile (3.9) ($\alpha = 0.65$) in the lower layer, the (dimensional) e-folding times are 6.6 months, 8.9 months, and 14.4 years, respectively.

Thus, one of the rings is virtually stable, whereas the lifespan of the other two is sufficiently large to fit with, at least, some observations.

3.3. *Discussion: the mechanism of stabilization*

Dewar & Killworth (1995) interpreted the stabilization of vortices with co-rotating deep flow through an energy analysis of the linearized problem. They showed that

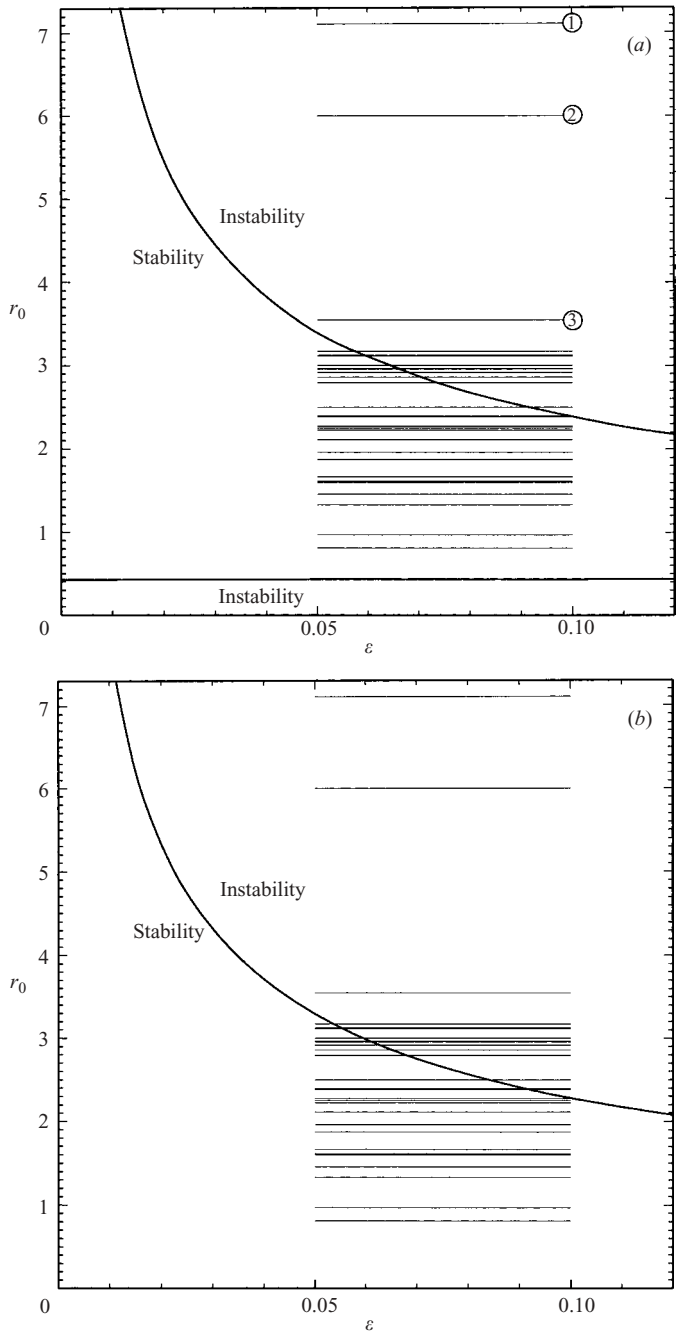

FIGURE 4. Stability of non-compensated vortices with respect to the first mode of $k = 2$. In the upper layer, the vortex is determined by (3.2), (3.3), or (3.4), and the lower-layer circulation determined by (3.9) with $\alpha = 0.65$. The notation is the same as in figure 2. (*a*) Gaussian vortex (the circles mark vortices with parameters (3.10)–(3.11)), (*b*) Algebraic vortex.

vertical shear of the vortex supports a flux of energy from the vortex to the disturbance ('baroclinic release'), whereas horizontal shear supports a flux from the disturbance to the vortex ('barotropic gain'). For compensated vortices, the former is much stronger

than the latter, which results in instability. A co-rotating deep circulation, in turn, causes a sharp increase in the barotropic gain – until it matches the baroclinic release and, thus, stabilizes the vortex.

There is little doubt that a similar analysis would yield similar results for the present case. To begin with, the present compensated vortices are exactly the same as those considered by Dewar & Killworth (1995), and the baroclinic release for them must exceed the barotropic gain. For vortices with uniform lower-layer PV, in turn, the two fluxes must be equal (because of stability). Hence, in our case and that of Dewar & Killworth (1995), the dependence of the energy fluxes on the amplitude of the deep flow must be very similar, even though the profiles of the deep flow are different. In other words, the stabilization of vortices with uniform PV in the lower layer – just like any other vortices with co-rotating deep circulation – occurs due to a balance of baroclinic release of energy and its barotropic gain.

The above interpretation can be reinforced by observing that condition (3.7) of uniformity of lower-layer PV can be viewed as a requirement that horizontal shear be as strong as vertical shear. In particular, vortices with radii larger than the deformation radius, for which the first term in (3.7) tends to zero, can be stable only if the vertical shear (second and third terms) is also small. Physically, this implies that the velocity field of large oceanic rings should decay slower with depth (and thus penetrate deeper) than that of smaller rings.

An alternative (simpler) interpretation is based on representation of the unstable disturbance by two phase-locked Rossby waves, rotating around the vortex in the upper and lower layers. Then, if the lower-layer PV gradient is zero, it cannot support the corresponding wave, and the instability is inhibited.

3.4. *Discussion: do vortices with* $\alpha \neq 1$ *have physical meaning?*

To answer this subsection's title question, recall that most oceanic rings are shed by frontal currents. When a ring separates from the current and arrives at a new location, it displaces the interface and thus forces the lower layer to spin up (otherwise the lower-layer particles would not preserve their PV). This scenario, however, does not take into account friction – which can slow down the spin-up and prevent the lower layer from reaching the swirl velocity prescribed by the condition of constant PV. Circulation (3.9) with $\alpha < 1$ appears to be a good model for such cases.

Generally, the case $\alpha < 1$ can be viewed as a simple model of any non-uniformities of PV in the lower layer, including those that are caused by background currents (which are often present in the 'real' ocean). The existence of stable vortices with $\alpha < 1$ demonstrates the robustness of the suggested mechanism and shows that stability persists in the face of less than ideal conditions.

Finally, note that deep flow (3.9) is not the only possibility to stabilize the vortex: Dewar & Killworth (1995) showed that a co-rotating Gaussian circulation has the same effect. Our point is that (3.9) stabilizes the vortex and appears to be a realistic model of oceanic rings. It should be emphasized, however, that full validation of the hypothesis on uniform lower-layer PV should include analysis of the PV field of 'real' oceanic rings.

4. Asymptotic results: formulation of the problem

Assume that the upper layer is much thinner than the lower layer,

$$\varepsilon \ll 1,$$

and that the flow in the latter is weak, say, $V_2 = \mathrm{O}(\varepsilon)$ (it may or may not correspond to constant PV, as we shall first consider the general case). Accordingly,

$$V_2 = \varepsilon \tilde{V}_2,$$

where $\tilde{V}_2 = \mathrm{O}(1)$. Rewriting equations (2.4)–(2.5) in terms of $\tilde{V}_2$ and omitting the tildes, we obtain

$$(cr - V_1)\left[\frac{1}{r}\frac{\mathrm{d}}{\mathrm{d}r}\left(r\frac{\mathrm{d}\psi_1}{\mathrm{d}r}\right) - \frac{k^2}{r^2}\psi_1 - \psi_1 + \psi_2\right] + \left\{\frac{\mathrm{d}}{\mathrm{d}r}\left[\frac{1}{r}\frac{\mathrm{d}}{\mathrm{d}r}(rV_1)\right] - V_1 + \varepsilon V_2\right\}\psi_1 = 0, \quad (4.1)$$

$$(cr - \varepsilon V_2)\left[\frac{1}{r}\frac{\mathrm{d}}{\mathrm{d}r}\left(r\frac{\mathrm{d}\psi_2}{\mathrm{d}r}\right) - \frac{k^2}{r^2}\psi_2 - \varepsilon\psi_2 + \varepsilon\psi_1\right] + \varepsilon\left\{\frac{\mathrm{d}}{\mathrm{d}r}\left[\frac{1}{r}\frac{\mathrm{d}}{\mathrm{d}r}(rV_2)\right] - \varepsilon V_2 + V_1\right\}\psi_2 = 0. \quad (4.2)$$

Mathematically, the eigenvalue problem (4.1)–(4.2), (2.6) is similar to the one describing compensated vortices. The latter has been thoroughly examined in B03, which enables us to omit some of the technical details and present only the conclusions. In particular, one can readily show that (4.1)–(4.2), (2.6) admit three types of modes:

1. lower-layer-dominated (LLD) modes, for which

$$\psi_1 = \mathrm{O}(1), \qquad \psi_2 = \mathrm{O}(1), \qquad c = \mathrm{O}(\varepsilon); \quad (4.3)$$

2. mixed (M) modes, for which

$$\psi_1 = \mathrm{O}(1), \qquad \psi_2 = \mathrm{O}(\varepsilon), \qquad c = \mathrm{O}(\varepsilon); \quad (4.4)$$

3. upper-layer-dominated (ULD, or equivalent-barotropic) modes, for which

$$\psi_1 = \mathrm{O}(1), \qquad \psi_2 = \mathrm{O}(\varepsilon), \qquad c = \mathrm{O}(1). \quad (4.5)$$

We shall assume (in all three cases) that, for $k = 1$, the leading-order c is non-zero, which eliminates the trivial solution

$$c = 0, \qquad \psi_1 = V_1, \qquad \psi_2 = \varepsilon V_2 \qquad \text{for } k = 1. \quad (4.6)$$

Equation (4.6) corresponds to an infinitesimal shift of the vortex as a whole and has nothing to do with its stability.

5. Asymptotic results: the analysis

In this section, the three types of modes defined above will be examined asymptotically. Non-mathematically minded readers can jump to the next section, where the asymptotic results will be summarized.

5.1. *Lower-layer-dominated modes*

Estimates (4.3) suggest the following expansions:

$$\psi_1 = \psi_1^{(0)} + \varepsilon\psi_1^{(1)} + \cdots, \qquad \psi_2 = \psi_2^{(0)} + \varepsilon\psi_2^{(1)} + \cdots, \qquad c = \varepsilon c^{(1)} + \cdots.$$

Then, (4.1)–(4.2), (2.6) yield

$$-V_1\left[\frac{1}{r}\frac{\mathrm{d}}{\mathrm{d}r}\left(r\frac{\mathrm{d}\psi_1^{(0)}}{\mathrm{d}r}\right) - \frac{k^2}{r^2}\psi_1^{(0)} - \psi_1^{(0)} + \psi_2^{(0)}\right] + \left\{\frac{\mathrm{d}}{\mathrm{d}r}\left[\frac{1}{r}\frac{\mathrm{d}}{\mathrm{d}r}(rV_1)\right] - V_1\right\}\psi_1^{(0)} = 0, \quad (5.1)$$

$$\psi_1^{(0)}(0) = \psi_1^{(0)}(\infty) = 0, \tag{5.2}$$

$$\left(c^{(1)}r - V_2\right)\left[\frac{1}{r}\frac{\mathrm{d}}{\mathrm{d}r}\left(r\frac{\mathrm{d}\psi_2^{(0)}}{\mathrm{d}r}\right) - \frac{k^2}{r^2}\psi_2^{(0)}\right] + \left\{\frac{\mathrm{d}}{\mathrm{d}r}\left[\frac{1}{r}\frac{\mathrm{d}}{\mathrm{d}r}(rV_2)\right] + V_1\right\}\psi_2^{(0)} = 0, \tag{5.3}$$

$$\psi_2^{(0)}(0) = \psi_2^{(0)}(\infty) = 0. \tag{5.4}$$

Observe that the lower-layer problem (5.3)–(5.4) is no longer coupled to the upper layer and can be solved independently. Hence, the leading-order eigenvalue $c^{(1)}$ depends only on the deep flow and curvature of the interface, and is independent of the upper-layer PV field. Furthermore, the upper-layer disturbance is 'enslaved' by its lower-layer counterpart (observe that the term $-V_1\psi_2^{(0)}$ in equation (5.1) plays the role of forcing).

The following theorem can be proved for equations (5.1)–(5.4):

THEOREM 1. *The boundary-value problem* (5.1)–(5.4) *does not have non-trivial* ($c^{(1)} \neq 0$) *solutions for* $k = 1$,

i.e. LLD-modes do not exist for the first azimuthal wavenumber (the proof of this theorem can be found in Appendix B). It can be further proved that:

THEOREM 2. *If*

$$Q_2'^{(1)} = \frac{\mathrm{d}}{\mathrm{d}r}\left[\frac{1}{r}\frac{\mathrm{d}}{\mathrm{d}r}(rV_2)\right] + V_1$$

never changes sign, the eigenvalue problem (5.3)–(5.4) *does not have complex* (*unstable*) *eigenvalues*,

which is the usual sufficient stability criterion for flows with monotonic PV (Dritschel 1988).

Theorem 2 appears to supply examples of vortices which are stable with respect to LLD-modes. It remains to be seen whether these vortices are stable with respect to the other two types of modes.

5.2. *Mixed modes*

In this case, the expansion of ψ_2 should start from an $\mathrm{O}(\varepsilon)$ term (see (4.4)),

$$\psi_1 = \psi_1^{(0)} + \varepsilon\psi_1^{(1)} + \cdots, \qquad \psi_2 = \varepsilon\psi_2^{(1)} + \cdots, \qquad c = \varepsilon c^{(1)} + \cdots.$$

Unlike the previous case (where it was sufficient to consider the leading order only), here we need to examine two orders of the eigenvalue problem (4.1)–(4.2), (2.6),

$$-V_1\left[\frac{1}{r}\frac{\mathrm{d}}{\mathrm{d}r}\left(r\frac{\mathrm{d}\psi_1^{(0)}}{\mathrm{d}r}\right) - \frac{k^2}{r^2}\psi_1^{(0)} - \psi_1^{(0)}\right] + \left\{\frac{\mathrm{d}}{\mathrm{d}r}\left[\frac{1}{r}\frac{\mathrm{d}}{\mathrm{d}r}(rV_1)\right] - V_1\right\}\psi_1^{(0)} = 0, \tag{5.5}$$

$$\psi_1^{(0)}(0) = \psi_1^{(0)}(\infty) = 0, \tag{5.6}$$

$$c^{(1)}r\left[\frac{1}{r}\frac{\mathrm{d}}{\mathrm{d}r}\left(r\frac{\mathrm{d}\psi_1^{(0)}}{\mathrm{d}r}\right) - \frac{k^2}{r^2}\psi_1^{(0)} - \psi_1^{(0)}\right] - V_1\left[\frac{1}{r}\frac{\mathrm{d}}{\mathrm{d}r}\left(r\frac{\mathrm{d}\psi_1^{(1)}}{\mathrm{d}r}\right) - \frac{k^2}{r^2}\psi_1^{(1)} - \psi_1^{(1)} + \psi_2^{(1)}\right] + \left\{\frac{\mathrm{d}}{\mathrm{d}r}\left[\frac{1}{r}\frac{\mathrm{d}}{\mathrm{d}r}(rV_1)\right] - V_1\right\}\psi_1^{(1)} + V_2\psi_1^{(0)} = 0, \tag{5.7}$$

$$\psi_1^{(1)}(0) = \psi_1^{(1)}(\infty) = 0, \tag{5.8}$$

$$\left(c^{(1)}r - V_2\right)\left[\frac{1}{r}\frac{\mathrm{d}}{\mathrm{d}r}\left(r\frac{\mathrm{d}\psi_2^{(1)}}{\mathrm{d}r}\right) - \frac{k^2}{r^2}\psi_2^{(1)} + \psi_1^{(0)}\right] + \left\{\frac{\mathrm{d}}{\mathrm{d}r}\left[\frac{1}{r}\frac{\mathrm{d}}{\mathrm{d}r}(rV_2)\right] + V_1\right\}\psi_2^{(1)} = 0, \tag{5.9}$$

$$\psi_2^{(1)}(0) = \psi_2^{(1)}(\infty) = 0. \tag{5.10}$$

It can be demonstrated (see Appendix B) that,

THEOREM 3. *The boundary-value problem* (5.5)–(5.6) *has a solution only for* $k = 1$, *in which case*

$$\psi_1^{(0)} = V_1, \tag{5.11}$$

i.e. M-modes exist only for the first azimuthal wavenumber and, in this respect, complement LLD-modes. Observe also that (5.11) brings us dangerously close to the meaningless trivial solution (compare (5.11) with (4.6)). Thus, to eliminate the trivial solution, we shall have to ensure that $c^{(1)} \neq 0$.

Before formulating the next theorem, observe that $\psi_1^{(1)}$ can be eliminated from the first-order set (5.7)–(5.10). Indeed, integrate (5.7) over $0 < r < \infty$. Integrating by parts (twice), using the boundary conditions (5.8), and takin into account (5.11), we obtain

$$\int_0^\infty rV_1\left(c^{(1)}r - V_2\right)\mathrm{d}r + \int_0^\infty rV_1\psi_2^{(1)}\,\mathrm{d}r = 0. \tag{5.12}$$

Finally, put $k = 1$ and substitute (5.11) into (5.9),

$$\left(c^{(1)}r - V_2\right)\left[\frac{1}{r}\frac{\mathrm{d}}{\mathrm{d}r}\left(r\frac{\mathrm{d}\psi_2^{(1)}}{\mathrm{d}r}\right) - \frac{1}{r^2}\psi_2^{(1)} + V_1\right] + \left\{\frac{\mathrm{d}}{\mathrm{d}r}\left[\frac{1}{r}\frac{\mathrm{d}}{\mathrm{d}r}(rV_2)\right] + V_1\right\}\psi_2^{(1)} = 0. \tag{5.13}$$

Equations (5.10) and (5.12)–(5.13) form an eigenvalue problem, where $c^{(1)}$ is the eigenvalue and $\psi_2^{(1)}$ is the eigenfunction.

THEOREM 4. *If*

$$Q_2^{\prime(1)} = \frac{\mathrm{d}}{\mathrm{d}r}\left[\frac{1}{r}\frac{\mathrm{d}}{\mathrm{d}r}(rV_2)\right] + V_1 \qquad \text{and} \qquad V_1$$

never change sign, and

$$Q_2^{\prime(1)}V_1 \leqslant 0,$$

problem (5.10), (5.12)–(5.13) *does not have complex* (*unstable*) *eigenvalues.*

(The proof of this theorem can be found in Appendix B.)

Observe that Theorem 4 requires stronger conditions for stability than its LLD counterpart (Theorem 2): if the former holds, the latter holds as well.

5.3. *Upper-layer-dominated modes*

In this case, estimates (4.5) suggest the following expansions:

$$\psi_1 = \psi_1^{(0)} + \varepsilon\psi_1^{(1)} + \cdots, \qquad \psi_2 = \varepsilon\psi_2^{(1)} + \cdots, \qquad c = c^{(0)} + \cdots.$$

Then, to the leading order, the upper layer decouples from the lower layer and is described by the standard eigenvalue problem for equivalent-barotropic vortices,

$$\left(c^{(0)}r - V_1\right)\left[\frac{1}{r}\frac{\mathrm{d}}{\mathrm{d}r}\left(r\frac{\mathrm{d}\psi_1^{(0)}}{\mathrm{d}r}\right) - \frac{k^2}{r^2}\psi_1^{(0)} - \psi_1^{(0)}\right] + \left\{\frac{\mathrm{d}}{\mathrm{d}r}\left[\frac{1}{r}\frac{\mathrm{d}}{\mathrm{d}r}(rV_1)\right] - V_1\right\}\psi_1^{(0)} = 0, \tag{5.14}$$

$$\psi_1^{(0)}(0) = \psi_1^{(0)}(\infty) = 0 \tag{5.15}$$

(the lower-layer equations are omitted as they are not needed).

The following theorems can be proved:

THEOREM 5. *The eigenvalue problem* (5.14)–(5.15) *does not have non-trivial* ($c^{(0)} \neq 0$) *solutions for* $k = 1$.

THEOREM 6. *If*

$$Q_1'^{(0)} = \frac{\mathrm{d}}{\mathrm{d}r}\left[\frac{1}{r}\frac{\mathrm{d}}{\mathrm{d}r}(rV_1)\right] - V_1$$

never changes sign, problem (5.14)–(5.15) *does not have complex* (*unstable*) *eigenvalues.*

Theorem 5 has been formulated by Paldor (1999), and Theorem 6 is a particular case of Dritschel's (1988) general result.

6. Asymptotic results: discussion and summary

Thus, we have developed a seemingly complete asymptotic description of stability of oceanic vortices. This description, however, is based on leading-order approximations, and it is unclear whether a neutrally stable (to the leading order) vortex will remain stable within the framework of higher-order approximations.

For compensated vortices, the answer to this question has been given in B03: higher-order corrections to a real leading-order eigenvalue are either complex or do not exist at all. The former means weak instability, whereas the latter should be interpreted as stability (since absence of unstable modes *is* stability).

Unfortunately, extension of the higher-order results of B03 to non-compensated vortices turned out to be a difficult task – there are cases, however, where it can be bypassed. Assume, for example, that the leading-order equations do not have solutions. Then, surely, the question of higher-order corrections is irrelevant, as there are no neutrally stable eigenvalues that can be made unstable. In this case, neither stable nor unstable solutions exist, which means stability.

We are now ready to summarize the asymptotic results obtained:

1. If the asymptotic eigenvalue problems for LLD- and M-modes ((5.3)–(5.4) and (5.10), (5.12)–(5.13), respectively) have one or more complex eigenvalues, the vortex is unstable, and the non-dimensional growth rate is $k\,\mathrm{Im}\,c = \mathrm{O}(\varepsilon)$.

2. If the asymptotic problem for ULD-modes, (5.14)–(5.15), has one or more complex eigenvalues, the vortex is unstable, and the growth rate is $k\mathrm{Im}\,c = \mathrm{O}(1)$.

3. If the three asymptotic problems have non-trivial ($c \neq 0$) real eigenvalues, but no complex ones, no definitive conclusion can be drawn. The vortex can be either stable or weakly unstable (due to higher-order corrections).

4. If the three asymptotic problems have neither complex nor non-trivial real eigenvalues, the vortex is stable.

In the next section, we shall demonstrate that vortices with uniform PV in the lower layer fall into the fourth category.

7. Asymptotic results: vortices with uniform PV in the lower layer

Consider the eigenvalue problem (5.3)–(5.4) for LLD-modes and assume

$$\frac{\mathrm{d}}{\mathrm{d}r}\left[\frac{1}{r}\frac{\mathrm{d}}{\mathrm{d}r}\left(rV_2\right)\right]+V_1=0 \tag{7.1}$$

(which is what the condition of constant lower-layer PV amounts to at the leading order). Then, (5.3) becomes

$$\frac{1}{r}\frac{\mathrm{d}}{\mathrm{d}r}\left(r\frac{\mathrm{d}\psi_2^{(0)}}{\mathrm{d}r}\right)-\frac{k^2}{r^2}\psi_2^{(0)}=0.$$

One can readily see that this equation has no bounded solutions.

Next, substitute (7.1) into the M-mode equation (5.13) and rewrite the latter as

$$\frac{\mathrm{d}}{\mathrm{d}r}\left[\frac{1}{r}\frac{\mathrm{d}}{\mathrm{d}r}\left(r\psi_2^{(1)}\right)\right]+V_1=0.$$

Comparing this equation with (7.1), one can deduce that

$$\psi_2^{(1)}=V_2+Ar^k+Br^{-k}. \tag{7.2}$$

To satisfy the boundary conditions (5.10), put

$$A=0, \qquad B=0. \tag{7.3}$$

Finally, we substitute (7.2)–(7.3) into the integral condition (5.12) and obtain

$$c^{(1)}\int_0^\infty r^2V_1\,\mathrm{d}r=0. \tag{7.4}$$

Since the net upper-layer angular momentum is non-zero (see (2.7)), it follows from (7.4) that $c^{(1)}=0$ (which is the trivial solution and should be discarded).

Thus, for monopolar vortices with uniform PV in the lower layer, the M-problem admits only the trivial solution, and the LLD-problem does not admit any solutions at all. We conclude that vortices with uniform PV are baroclinically stable.

The ULD-modes are not sensitive to deep flow (observe that V_2 does not appear in equation (5.14)). As a result, barotropic stability of a vortex is determined by its profile in the upper layer, and the condition of constant lower-layer PV is unimportant in this case. We shall not discuss ULD-modes in more detail, as barotropic effects play no part in the instability of mesoscale rings (recall that, out of the three vortex profiles considered, only the Gaussian profile was barotropically unstable and, even in this case, none of the 'real' rings fell into the region of barotropic instability – see figures 2*a*, 4*a*).

8. Ageostrophic vortices

8.1. *Formulation of the problem*

In this case, the flow is described by the layer depths h_{*j}, pressures p_{*j}, the radial velocities u_{*j}, and the azimuthal velocities v_{*j} (where $j=1,2$ is the layer number

and asterisks mark the dimensional variables). We shall introduce the following non-dimensional variables:

$$t = ft_*, \qquad (x, y) = \frac{(x_*, y_*)}{L_d}, \qquad u_j = \frac{u_{*j}}{fL_d}, \qquad v_j = \frac{v_{*j}}{fL_d},$$
$$h_1 = \frac{h_{*1}}{H_{*1}}, \qquad h_2 = \frac{h_{*2}}{H_{*2}}, \qquad p_j = \frac{p_{*j}}{\rho_0 g' H_{*1}},$$

where H_{*j} are the layer characteristic depths, L_d is the deformation radius based on H_{*1}, ρ_0 is the mean density of water, and g' is the reduced acceleration due to gravity. Then, the non-dimensional equations governing ageostrophic vortices on the f-plane are

$$\frac{\partial u_j}{\partial t} + u_j \frac{\partial u_j}{\partial r} + \frac{1}{r} v_j \left(\frac{\partial u_j}{\partial \theta} - v_j \right) + \frac{\partial p_j}{\partial r} = v_j, \tag{8.1}$$

$$\frac{\partial v_j}{\partial t} + u_j \frac{\partial v_j}{\partial r} + \frac{1}{r} v_j \left(\frac{\partial v_j}{\partial \theta} + u_j \right) + \frac{1}{r} \frac{\partial p_j}{\partial \theta} = -u_j, \tag{8.2}$$

$$r \frac{\partial h_j}{\partial t} + \frac{\partial}{\partial r}(r u_j h_j) + \frac{\partial}{\partial \theta}(v_j h_j) = 0, \tag{8.3}$$

$$p_2 = p_1 - h_1, \qquad \varepsilon h_1 + h_2 = 1 + \varepsilon, \tag{8.4}$$

where, as before, $\varepsilon = H_{*1}/H_{*2}$. Following the usual scheme of linear stability analysis, we represent the solution as a superposition of a steady state (vortex) and a small disturbance,

$$u_j(r, \theta, t) = u'_j(r, \theta, t), \qquad v_j(r, \theta, t) = V_j(r) + v'_j(r, \theta, t), \tag{8.5}$$

$$p_j(r, \theta, t) = P_j(r) + p'_j(r, \theta, t), \qquad h_j(r, \theta, t) = H_j(r) + h'_j(r, \theta, t), \tag{8.6}$$

where the vortex satisfies the cyclostrophic, hydrostatic, and kinematic relations,

$$\frac{\mathrm{d}P_j}{\mathrm{d}r} = V_j + \frac{1}{r} V_j^2, \qquad P_2 = P_1 - H_1, \qquad \varepsilon H_1 + H_2 = 1 + \varepsilon. \tag{8.7}$$

Substituting (8.5)–(8.7) into (8.1)–(8.4) and omitting nonlinear terms, we obtain

$$\frac{\partial u'_j}{\partial t} + \frac{1}{r} V_j \left(\frac{\partial u'_j}{\partial \theta} - v'_j \right) - \frac{1}{r} v'_j V_j + \frac{\partial p'_j}{\partial r} = v'_j, \tag{8.8}$$

$$\frac{\partial v'_j}{\partial t} + u'_j \frac{\mathrm{d}V_j}{\mathrm{d}r} + \frac{1}{r} V_j \left(\frac{\partial v'_j}{\partial \theta} + u'_j \right) + \frac{1}{r} \frac{\partial p'_j}{\partial \theta} = -u'_j, \tag{8.9}$$

$$r \frac{\partial h'_j}{\partial t} + \frac{\partial}{\partial r}(r u'_j H_j) + \frac{\partial}{\partial \theta}(V_j h'_j + v'_j H_j) = 0, \tag{8.10}$$

$$p_2 = p_1 - h_1, \qquad \varepsilon h_1 + h_2 = 0. \tag{8.11}$$

As before, we are interested in normal modes,

$$u'_j(r, \theta, t) = \mathrm{Re}\left[u_j(r)\, \mathrm{e}^{\mathrm{i}k\theta - \mathrm{i}\omega t}\right], \qquad v'_j(r, \theta, t) = \mathrm{Re}\left[v_j(r)\, \mathrm{e}^{\mathrm{i}k\theta - \mathrm{i}\omega t}\right], \tag{8.12}$$

$$p'_j(r, \theta, t) = \mathrm{Re}\left[p_j(r)\, \mathrm{e}^{\mathrm{i}k\theta - \mathrm{i}\omega t}\right], \qquad h'_j(r, \theta, t) = \mathrm{Re}\left[h_j(r)\, \mathrm{e}^{\mathrm{i}k\theta - \mathrm{i}\omega t}\right], \tag{8.13}$$

where ω is the frequency (which shall use it instead of $c = \omega/k$). Substitution of (8.12)–(8.13) into (8.8)–(8.11) yields

$$\mathrm{i}\left(\frac{k}{r} V_j - \omega \right) u_j - \left(1 + \frac{2}{r} V_j \right) v_j + \frac{\mathrm{d}p_j}{\mathrm{d}r} = 0, \tag{8.14}$$

$$\mathrm{i}\left(\frac{k}{r}V_j-\omega\right)v_j+\left(1+\frac{1}{r}V_j+\frac{\mathrm{d}V_j}{\mathrm{d}r}\right)u_j+\frac{\mathrm{i}k}{r}p_j=0, \tag{8.15}$$

$$\mathrm{i}\left(\frac{k}{r}V_j-\omega\right)h_j+\frac{1}{r}\frac{\mathrm{d}}{\mathrm{d}r}(rH_ju_j)+\frac{\mathrm{i}k}{r}H_jv_j=0, \tag{8.16}$$

$$p_2=p_1-h_1,\qquad \varepsilon h_1+h_2=0. \tag{8.17}$$

Next, it is convenient to eliminate the lower-layer velocities u_2, v_2. Using ((8.14)–(8.15))$_{j=2}$ to express them through p_2,

$$u_2=-\mathrm{i}\frac{\left(\frac{k}{r}V_2-\omega\right)\frac{\mathrm{d}p_2}{\mathrm{d}r}+\left(1+\frac{2}{r}V_2\right)\frac{k}{r}p_2}{\left(1+\frac{1}{r}V_2+\frac{\mathrm{d}V_2}{\mathrm{d}r}\right)\left(1+\frac{2}{r}V_2\right)-\left(\frac{k}{r}V_2-\omega\right)^2},$$

$$v_2=\frac{\left(1+\frac{1}{r}V_2+\frac{\mathrm{d}V_2}{\mathrm{d}r}\right)\frac{\mathrm{d}p_2}{\mathrm{d}r}+\left(\frac{k}{r}V_2-\omega\right)\frac{k}{r}p_2}{\left(1+\frac{1}{r}V_2+\frac{\mathrm{d}V_2}{\mathrm{d}r}\right)\left(1+\frac{2}{r}V_2\right)-\left(\frac{k}{r}V_2-\omega\right)^2},$$

we substitute these expressions into (8.16)$_{j=2}$. After cumbersome calculations, we obtain

$$\frac{\mathrm{d}}{\mathrm{d}r}\left(rF_2\frac{\mathrm{d}p_2}{\mathrm{d}r}\right)+\left\{\frac{\frac{\mathrm{d}}{\mathrm{d}r}\left[\frac{k}{r}(r+2V_2)F_2\right]}{\frac{k}{r}V_2-\omega}-\frac{k^2}{r}F_2\right\}p_2-rh_2=0, \tag{8.18}$$

where

$$F_2=\frac{H_2}{\left(1+\frac{1}{r}V_2+\frac{\mathrm{d}V_2}{\mathrm{d}r}\right)\left(1+\frac{2}{r}V_2\right)-\left(\frac{k}{r}V_2-\omega\right)^2}. \tag{8.19}$$

Assume now that the flow in the lower layer is weak,

$$V_2=\varepsilon\tilde{V}_2,\qquad P_2=\varepsilon\tilde{P}_2. \tag{8.20}$$

Substituting (8.20) into ((8.14)–(8.16))$_{j=1}$, (8.17), (8.18)–(8.19), and (8.7), we obtain the following set of ODEs (tildes omitted):

$$\mathrm{i}\left(\frac{k}{r}V_1-\omega\right)u_1-\left(1+\frac{2}{r}V_1\right)v_1+\frac{\mathrm{d}h_1}{\mathrm{d}r}+\frac{\mathrm{d}p_2}{\mathrm{d}r}=0, \tag{8.21}$$

$$\mathrm{i}\left(\frac{k}{r}V_1-\omega\right)v_1+\left(1+\frac{1}{r}V_1+\frac{\mathrm{d}V_1}{\mathrm{d}r}\right)u_1+\frac{\mathrm{i}k}{r}(h_1+p_2)=0, \tag{8.22}$$

$$\mathrm{i}r\left(\frac{k}{r}V_1-\omega\right)h_1+\frac{\mathrm{d}}{\mathrm{d}r}(rH_1u_1)+\mathrm{i}kH_1v_1=0, \tag{8.23}$$

$$\frac{\mathrm{d}}{\mathrm{d}r}\left(rF_2\frac{\mathrm{d}p_2}{\mathrm{d}r}\right)+\left\{\frac{\frac{\mathrm{d}}{\mathrm{d}r}\left[\frac{k}{r}(r+2\varepsilon V_2)F_2\right]}{\frac{k}{r}\varepsilon V_2-\omega}-\frac{k^2}{r}F_2\right\}p_2+\varepsilon rh_1=0, \tag{8.24}$$

where

$$F_2 = \frac{1+\varepsilon-\varepsilon H_1}{\left(1+\frac{1}{r}\varepsilon V_2+\varepsilon\frac{\mathrm{d}V_2}{\mathrm{d}r}\right)\left(1+\frac{2}{r}\varepsilon V_2\right)-\left(\frac{k}{r}\varepsilon V_2-\omega\right)^2}, \tag{8.25}$$

$$\frac{\mathrm{d}H_1}{\mathrm{d}r} = V_1+\frac{1}{r}V_1^2-\varepsilon\left(V_2+\frac{1}{r}\varepsilon V_2^2\right), \tag{8.26}$$

These equations should be supplemented by the smoothness conditions at the centre of the vortex,

$$\mathrm{i}kv_1+u_1=0, \qquad h_1=0, \qquad p_2=0 \qquad \text{at} \qquad r=0, \tag{8.27}$$

which can be obtained by expanding equations (8.22) and (8.23) about $r=0$. We shall also impose the boundedness conditions at infinity,

$$u_1, v_1, h_1, p_2 \to 0 \qquad \text{as} \qquad r\to\infty. \tag{8.28}$$

Equations (8.21)–(8.28) form an eigenvalue problem, where ω is the eigenvalue.

8.2. *Discussion*

Observe that the lower-layer part of the equations derived, (8.24)–(8.25), has small parameters in exactly the same places as the quasi-geostrophic approximation.† As a result of this similarity, all QG conclusions obtained for LLD-modes (§ 5.1) remain intact. In particular, straightforward calculations show that the ageostrophic LLD-problem differs from (5.3)–(5.4) only in notation: $\psi_2 \to p_2$. Accordingly, the conclusion regarding the stability of vortices with constant lower-layer PV with respect to LLD-modes holds for the ageostrophic case as well.

The upper-layer equations (8.21)–(8.23), (8.26), in turn, differ significantly from their QG counterparts – but this is unimportant, as equivalent-barotropic effects are negligible for instability of mesoscale rings (it is implied here that ageostrophy does not change barotropic effects too much).

Thus, we only need to clarify how ageostrophy affects M-modes (non-mathematically minded readers can jump to the next section).

8.3. *Mixed modes*

The asymptotic expansion for this case is

$$u_1 = u_1^{(0)}+\varepsilon u_1^{(1)}+\cdots, \qquad v_1 = v_1^{(0)}+\varepsilon v_1^{(1)}+\cdots, \qquad h_1 = h_1^{(0)}+\varepsilon h_1^{(1)}+\cdots,$$
$$p_2 = \varepsilon p_2^{(1)}+\cdots, \qquad H_1 = H_1^{(0)}+\varepsilon H_1^{(1)}+\cdots, \qquad \omega = \varepsilon\omega^{(1)}+\cdots.$$

Then, the first two orders of equations (8.21)–(8.26) yield

$$\frac{\mathrm{i}k}{r}V_1u_1^{(0)}-\left(1+\frac{2}{r}V_1\right)v_1^{(0)}+\frac{\mathrm{d}h_1^{(0)}}{\mathrm{d}r}=0, \tag{8.29}$$

$$\frac{\mathrm{i}k}{r}V_1v_1^{(0)}+\left(1+\frac{1}{r}V_1+\frac{\mathrm{d}V_1}{\mathrm{d}r}\right)u_1^{(0)}+\frac{\mathrm{i}k}{r}h_1^{(0)}=0, \tag{8.30}$$

† Physically, quasi-geostrophy of the lower layer follows from the smallness of the displacement of the interface (in comparison with H_2), and the weakness of the lower-layer flow. Note also, that the upper-layer flow may remain ageostrophic, as the displacement of the interface can be comparable to H_1.

$$\mathrm{i}kV_1h_1^{(0)} + \frac{\mathrm{d}}{\mathrm{d}r}\left(rH_1^{(0)}u_1^{(0)}\right) + \mathrm{i}kH_1^{(0)}v_1^{(0)} = 0, \tag{8.31}$$

$$\mathrm{i}ku_1^{(0)} - v_1^{(0)} = 0, \qquad \mathrm{i}kv_1^{(0)} + u_1^{(0)} = 0, \qquad h_1^{(0)} = 0 \qquad \text{at} \qquad r = 0, \tag{8.32}$$

$$\frac{\mathrm{i}k}{r}V_1u_1^{(1)} - \mathrm{i}\omega^{(1)}u_1^{(0)} - \left(1 + \frac{2}{r}V_1\right)v_1^{(1)} + \frac{\mathrm{d}h_1^{(1)}}{\mathrm{d}r} + \frac{\mathrm{d}p_2^{(1)}}{\mathrm{d}r} = 0, \tag{8.33}$$

$$\frac{\mathrm{i}k}{r}V_1v_1^{(1)} - \mathrm{i}\omega^{(1)}v_1^{(0)} + \left(1 + \frac{1}{r}V_1 + \frac{\mathrm{d}V_1}{\mathrm{d}r}\right)u_1^{(1)} + \frac{\mathrm{i}k}{r}\left(h_1^{(1)} + p_2^{(1)}\right) = 0, \tag{8.34}$$

$$\mathrm{i}kV_1h_1^{(1)} - \mathrm{i}\omega^{(1)}rh_1^{(0)} + \frac{\mathrm{d}}{\mathrm{d}r}\left(rH_1^{(0)}u_1^{(1)} + rH_1^{(1)}u_1^{(0)}\right) + \mathrm{i}k\left(H_1^{(0)}v_1^{(1)} + H_1^{(1)}v_1^{(0)}\right) = 0, \tag{8.35}$$

$$\mathrm{i}ku_1^{(1)} - v_1^{(1)} = 0, \qquad \mathrm{i}kv_1^{(1)} + u_1^{(1)} = 0, \qquad h_1^{(1)} = 0 \qquad \text{at} \qquad r = 0, \tag{8.36}$$

$$\left(\frac{\omega^{(1)}r}{k} - V_2\right)\left[\frac{1}{r}\frac{\mathrm{d}}{\mathrm{d}r}\left(r\frac{\mathrm{d}p_2^{(1)}}{\mathrm{d}r}\right) - \frac{k^2}{r^2}p_2^{(1)} + h_1^{(0)}\right] + \left\{\frac{\mathrm{d}}{\mathrm{d}r}\left[\frac{1}{r}\frac{\mathrm{d}}{\mathrm{d}r}(rV_2)\right] + V_1\right\}p_2^{(1)} = 0, \tag{8.37}$$

$$p_2^{(1)} = 0 \qquad \text{at} \qquad r = 0, \tag{8.38}$$

where

$$\frac{\mathrm{d}H_1^{(0)}}{\mathrm{d}r} = V_1 + \frac{1}{r}V_1^2, \qquad \frac{\mathrm{d}H_1^{(1)}}{\mathrm{d}r} = -V_2. \tag{8.39}$$

Unfortunately, we have been unable to rigorously prove that the zeroth-order upper-layer eigenvalue problem (8.29)–(8.32) does not have a solution for $k \geqslant 2$ (which would be the ageostrophic equivalent of Theorem 3). However, we have carried out an extensive numerical study: for various vortex profiles, equations (8.29)–(8.32) were solved as an eigenvalue problem, with k being the eigenvalue. In all cases, the only solution found was $k = 1$. Hence, in what follows, we shall consider only the first azimuthal wavenumber.

It can be verified by inspection that the zeroth-order upper-layer problem (8.29)–(8.32), with $k = 1$, is satisfied by

$$u_1^{(0)} = -\frac{\mathrm{i}}{r}V_1, \qquad v_1^{(0)} = \frac{\mathrm{d}V_1}{\mathrm{d}r}, \qquad h_1^{(0)} = \frac{\mathrm{d}H_1^{(0)}}{\mathrm{d}r} \tag{8.40}$$

(which is the ageostrophic analogue of solution (5.11)). Substituting (8.40) and $k = 1$ into the first-order upper-layer equations, (8.33)–(8.36), we obtain

$$\frac{\mathrm{i}}{r}V_1u_1^{(1)} - \omega^{(1)}\frac{1}{r}V_1 - \left(1 + \frac{2}{r}V_1\right)v_1^{(1)} + \frac{\mathrm{d}h_1^{(1)}}{\mathrm{d}r} + \frac{\mathrm{d}p_2^{(1)}}{\mathrm{d}r} = 0, \tag{8.41}$$

$$\frac{\mathrm{i}}{r}V_1v_1^{(1)} - \mathrm{i}\omega^{(1)}\frac{\mathrm{d}V_1}{\mathrm{d}r} + \left(1 + \frac{1}{r}V_1 + \frac{\mathrm{d}V_1}{\mathrm{d}r}\right)u_1^{(1)} + \frac{\mathrm{i}}{r}\left(h_1^{(1)} + p_2^{(1)}\right) = 0, \tag{8.42}$$

$$\mathrm{i}V_1h_1^{(1)} - \mathrm{i}\omega^{(1)}r\frac{\mathrm{d}H_1^{(0)}}{\mathrm{d}r} + \frac{\mathrm{d}}{\mathrm{d}r}\left(rH_1^{(0)}u_1^{(1)} - \mathrm{i}H_1^{(1)}V_1\right) + \mathrm{i}\left(H_1^{(0)}v_1^{(1)} + H_1^{(1)}\frac{\mathrm{d}V_1}{\mathrm{d}r}\right) = 0, \tag{8.43}$$

$$\mathrm{i}u_1^{(1)} - v_1^{(1)} = 0, \qquad \mathrm{i}v_1^{(1)} + u_1^{(1)} = 0, \qquad h_1^{(1)} = 0. \tag{8.44}$$

Equations (8.41)–(8.44) form a non-homogeneous boundary-value problem for $u_1^{(1)}$, $v_1^{(1)}$, and $h_1^{(1)}$ – generally speaking, it only has a solution subject to a certain

orthogonality condition. To derive this condition, consider

$$\int_0^\infty \left[(8.41)\times \mathrm{i}r H_1^{(0)} + (8.42)\times r H_1^{(0)} + (8.43)\times (r+V_1)\right] \mathrm{d}r.$$

Cumbersome, but straightforward, calculations (involving integration by parts and use of (8.44), (8.39)) yield

$$\int_0^\infty (r+V_1)V_1\left(\omega^{(1)}r - V_2\right)\mathrm{d}r + \int_0^\infty (r+V_1)V_1 p_2^{(1)}\,\mathrm{d}r = 0. \tag{8.45}$$

Finally, substitute (8.40) and $k=1$ into the first-order lower-layer equation (8.37),

$$\left(\omega^{(1)}r - V_2\right)\left[\frac{1}{r}\frac{\mathrm{d}}{\mathrm{d}r}\left(r\frac{\mathrm{d}p_2^{(1)}}{\mathrm{d}r}\right) - \frac{k^2}{r^2}p_2^{(1)} + h_1^{(0)}\right] + \left\{\frac{\mathrm{d}}{\mathrm{d}r}\left[\frac{1}{r}\frac{\mathrm{d}}{\mathrm{d}r}(rV_2)\right] + V_1\right\} p_2^{(1)} = 0. \tag{8.46}$$

Comparing (8.45)–(8.46) with their QG counterparts (5.12)–(5.13), one can see that the latter follow from the former under the assumption $|V_1| \ll r$ (which is a part of the QG approximation), and change $p_2 \to \psi_2$, $\omega \to c$ (the latter is allowable because $k=1$).

It can be readily shown that, if

$$\frac{\mathrm{d}}{\mathrm{d}r}\left[\frac{1}{r}\frac{\mathrm{d}}{\mathrm{d}r}(rV_2)\right] + V_1 = 0,$$

the eigenvalue problem (8.45)–(8.46), (8.38) has no solution. Hence, ageostrophic vortices with uniform PV in the lower layer are stable with respect to M-modes.

9. Concluding remarks

We have examined the stability of oceanic rings with zero potential vorticity in the lower layer, with respect to harmonic disturbances (normal modes). Numerical solution of the exact quasi-geostrophic equations suggests that *barotropic* disturbances cannot destabilize mesoscale rings with realistic parameters, so our attention was mostly focused on the two types of *baroclinic* disturbances (lower-layer dominated and mixed modes, existing for $k \geqslant 2$ and $k=1$, respectively). These were examined for the QG case (numerically and asymptotically) and ageostrophic case (asymptotically). In both cases, rings with zero potential vorticity in the lower layer turned out to be stable, providing a model consistent with the observed lifespans of oceanic rings.

It should be emphasized that, everywhere in this paper, the upper layer of the ocean was assumed thin ($\varepsilon = H_1/H_2 \ll 1$), and the flow in the lower layer was assumed weak – which is inapplicable to, at least, some 'real' oceanic rings. Indeed, the depth ratio of the Southern Ocean rings might be as large as $\varepsilon \sim 1$, whereas some oceanic cold-core rings are localized 'in between' the upper and lower layers (and should be approximated by a three-layer model). In either case, uniform PV in the 'passive' layer(s) may or may not stabilize the ring, and these problems require a separate study.

Finally, we comment that the strong effect of a weak deep flow on vortices should not come as a surprise: the lower layer is thick, and its net characteristics (e.g. angular momentum) can be comparable to, or even exceed, those in the upper layer.

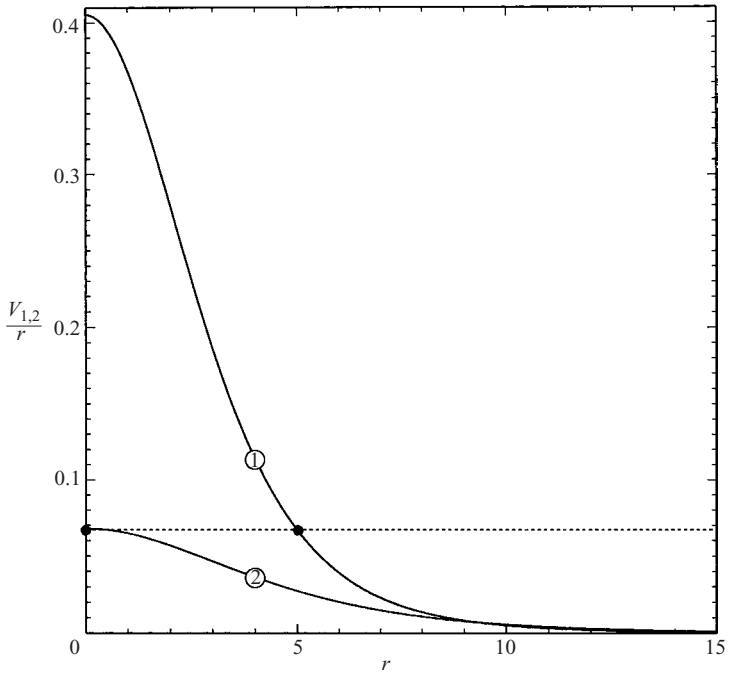

FIGURE 5. The locations of critical levels (shown by black circles) for a marginally stable ($\mathrm{Im}\, c = 0$) non-compensated vortex. The angular velocity profiles in the upper and lower layers are marked with 1 and 2, respectively. The dotted line shows the angular phase speed of the disturbance.

Appendix A. Computation of marginal stability curves for (2.4)–(2.6)

Unfortunately, the solution of the eigenvalue problem (2.4)–(2.6) is very difficult to compute for marginally stable ($\mathrm{Im}\, c = 0$), non-compensated vortices. The problem is that, in this case, the lower-layer critical level happens to be located at the centre of the vortex, i.e.

$$c = \lim_{r \to 0} \left\{ \frac{1}{r} V_2 \right\}$$

(see a schematic in figure 5). As a result, the coefficient of the highest-order derivative in equation (2.5) vanishes at $r = 0$, which is one of the endpoints of the path of integration. A similar singularity is associated with the upper-layer critical level, but it is located in one of the interior points – it can be bypassed by moving the path of integration into the plane of complex r (which is how the curves of marginal stability have been computed for compensated vortices, which have critical levels only in the upper layer – see B03).

Since we cannot compute the solution for marginally stable cases, we had to use the following extrapolation procedure:

1. Using a shooting method described in B03, four curves of equal growth rate, $\gamma = k\, \mathrm{Im}\, c$, on the (ε, r_0)-plane were computed, such that

$$\gamma = 0.0001,\ 0.0002,\ 0.0003,\ 0.0004 \qquad \text{(A 1)}$$

(see figure 6).

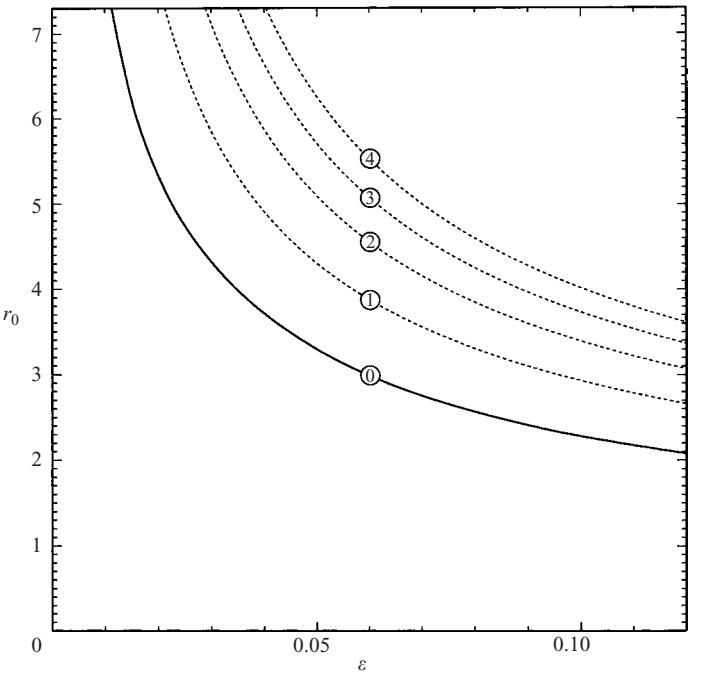

FIGURE 6. Curves of equal growth rate γ for non-compensated vortices, on the (ε, r_0)-plane. Curves 1–4 ($\gamma = 0.0001$, 0.0002, 0.0003, 0.0004) are computed using the eigenvalue problem (2.4)–(2.6), while curve 0 ($\gamma = 0$, the marginal stability curve) is obtained by extrapolating curves 1–4.

2. Since strongly varying curvature hampers extrapolation, curves (A 1) were redrawn in terms of new coordinates. This was done in two steps. First, we introduced

$$\varepsilon' = \frac{\hat{\varepsilon} - \varepsilon}{\Delta\varepsilon}, \qquad r_0' = \frac{\hat{r}_0 - r_0}{\Delta r_0}, \tag{A 2}$$

where $(\hat{\varepsilon}, \hat{r}_0)$ are the coordinates of a suitable centre on the (ε, r_0)-plane, and $\Delta\varepsilon$, Δr_0 are constants 'equilibrating' the scales of ε and r_0. We used

$$\hat{\varepsilon} = 0.12, \qquad \hat{r}_0 = 7.3$$

(which are the coordinates of the top right corner of figures 2, 4, 6). $\Delta\varepsilon$ and Δr_0 were chosen to ensure that all four curves would fit into the unit square $[0, 1] \times [0, 1]$ of the (ε', r_0')-plane. Secondly, we introduced polar coordinates (ϕ, R), such that

$$\varepsilon' = R\cos\phi, \qquad r_0' = R\sin\phi. \tag{A 3}$$

On the (ϕ, R)-plane, curves (A 1) look much flatter (see figure 7).

3. Next, the function $R(\gamma, \phi)$ was approximated by

$$R(\gamma, \phi) = A_0(\phi) + A_1(\phi)\,\gamma + A_2(\phi)\,\gamma^2 + A_3(\phi)\,\gamma^3, \tag{A 4}$$

where the coefficients $A_{0,1,2,3}$ were found by matching (A 4) to the four curves defined by (A 1). The marginal stability curve is then given by

$$R(0, \phi) = A_0(\phi). \tag{A 5}$$

4. Finally, curve (A 5) was 'moved' back to the (ε, r_0)-plane.

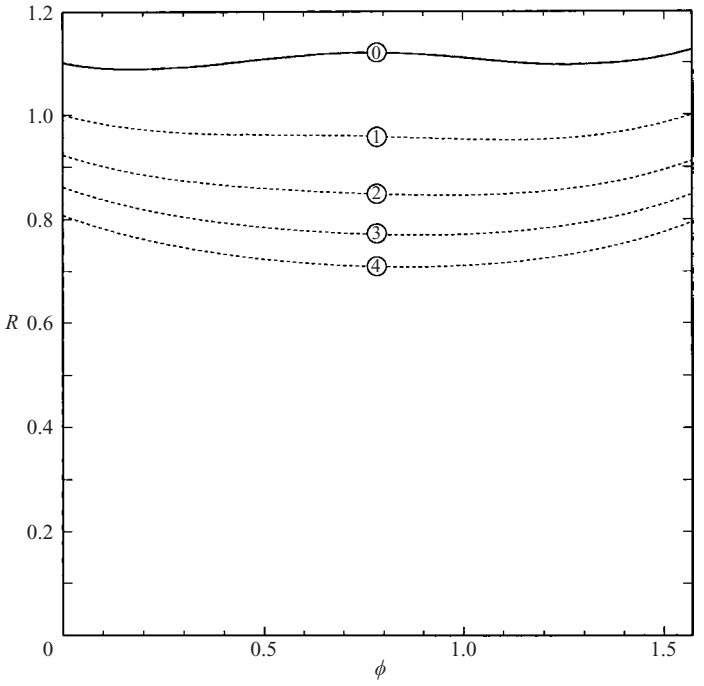

FIGURE 7. Curves of equal growth rate γ for non-compensated vortices, on the (ϕ, R)-plane (defined by (A 2)–(A 3)). The curves are marked similarly to figure 6.

Appendix B. Proofs of Theorems 1, 3, and 4

B.1. *Proof of Theorem* 1 (*non-existence of LLD-modes for* $k = 1$)

Multiply equation (5.1) by r and integrate with respect to r over $0 < r < \infty$. Integrating by parts, we obtain

$$\int_0^\infty \frac{k^2-1}{r} V_1 \psi_1^{(0)}\, \mathrm{d}r = \int_0^\infty r V_1 \psi_2^{(0)}\, \mathrm{d}r. \tag{B 1}$$

Then, multiply (5.3) by r^k and also integrate with respect to r. After cumbersome calculations, we obtain

$$\left[\left(c^{(1)}r - V_2\right) r^k \frac{\mathrm{d}\psi_2^{(0)}}{\mathrm{d}r} - r\psi_2^{(0)} \frac{\mathrm{d}}{\mathrm{d}r}\left(c^{(1)}r - V_2\right) r^{k-1}\right]_{r=0}^{r\to\infty} + \int_0^\infty \left[2(k-1)r^{k-2}\left(V_2 - \frac{\mathrm{d}V_2}{\mathrm{d}r}r\right) + r^k V_1\right] \psi_2^{(0)}\, \mathrm{d}r = 0. \tag{B 2}$$

It follows from the boundary conditions (5.4) and equation (5.3) that

$$\psi_2^{(0)} \to \mathrm{const}\, r^{-k} \qquad \text{at} \qquad r \to \infty,$$

or, without a loss of generality,

$$\psi_2^{(0)} \to r^{-k} \qquad \text{at} \qquad r \to \infty.$$

Then, (B 2) becomes

$$-2kc^{(1)} + \int_0^\infty \left[2(k-1)r^{k-2}\left(V_2 - \frac{\mathrm{d}V_2}{\mathrm{d}r}r\right) + r^k V_1\right]\psi_2^{(0)}\,\mathrm{d}r = 0. \tag{B 3}$$

Comparing (B 3) to (B 1) for $k=1$, we see that they are consistent only if $c^{(1)}=0$, which corresponds to the trivial solution (4.6) and should be discarded.

B.2. *Proof of Theorem* 3 (*non-existence of M-modes for* $k \geqslant 2$)

Put

$$\psi_1^{(0)} = V_1\chi \tag{B 4}$$

and rewrite (5.5)–(5.6) in terms of χ,

$$\frac{\mathrm{d}}{\mathrm{d}r}\left(rV_1^2\frac{\mathrm{d}\chi}{\mathrm{d}r}\right) - \frac{k^2-1}{r}V_1^2\chi = 0, \tag{B 5}$$

$$V_1\chi \to 0 \qquad \text{as} \qquad r \to 0, \infty. \tag{B 6}$$

Multiply (B 5) by χ^* and integrate over $0<r<\infty$. Integrating by parts (twice) and using (B 6), we obtain

$$\int_0^\infty V_1^2\left(r\left|\frac{\mathrm{d}\chi}{\mathrm{d}r}\right|^2 + \frac{k^2-1}{r}|\chi|^2\right)\mathrm{d}r = 0.$$

Clearly, if $k \geqslant 2$, then

$$\frac{\mathrm{d}\chi}{\mathrm{d}r} = 0, \qquad \chi = 0 \qquad \text{at all points where } V_1 \neq 0,$$

which makes χ zero everywhere (if a solution and its derivative of a second-order ODE with continuous coefficients are both zero at the same point, this solution is zero identically). If, however, $k=1$, the solution evidently exists: $\chi = \text{const}$. Putting const $=1$ and recalling (B 4), we obtain

$$\psi_1^{(0)} = V_1,$$

as required.

B.3. *Proof of Theorem* 4 (*stability criterion for M-modes*)

Multiply (5.13) by

$$\frac{r\psi_2^{(1)*}}{c^{(1)}r - V_2},$$

and integrate over $0<r<\infty$. Integrating by parts, using the boundary conditions (5.10), and taking the imaginary part, we obtain

$$\left(\operatorname{Im} c^{(1)}\right)\int_0^\infty \left(r^2V_1 - \frac{Q_2'^{(1)}}{\left|c^{(1)} - \frac{1}{r}V_2\right|^2}\left|\psi_2^{(1)}\right|^2\right)\mathrm{d}r = 0, \tag{B 7}$$

where

$$Q_2'^{(1)} = \frac{\mathrm{d}}{\mathrm{d}r}\left[\frac{1}{r}\frac{\mathrm{d}}{\mathrm{d}r}(rV_2)\right] + V_1$$

is the leading-order lower-layer PV gradient. One can see that, if V_1 and $Q_2'^{(1)}$ are sign-definite and $V_1 Q_2'^{(1)} \leqslant 0$, it follows from (B 7) that $\mathrm{Im}\, c^{(1)} = 0$ (stability).

REFERENCES

Benilov, E. S. 2003 Instability of quasigeostrophic vortices in a two-layer ocean with thin upper layer. *J. Fluid Mech.* **475**, 303–331 (referred to herein as B03).

Benilov, E. S., Broutman, D. & Kuznetsova, E. P. 1998 On the stability of large-amplitude vortices in a continuously stratified fluid on the f-plane. *J. Fluid Mech.* **355**, 139–162.

Carton, X. J. & McWilliams, J. C. 1989 Barotropic and baroclinic instabilities of axisymmetric vortices in a quasigeostrophic model. In *Mesoscale/Synoptic Coherent Structures in Geophysical Turbulence*. (ed. J. C. J. Nihoul & B. M. Jamart), pp. 225–244. Elsevier.

Dewar, W. K. & Killworth, P. D. 1995 On the stability of oceanic rings. *J. Phys. Oceanogr.* **25**, 1467–1487.

Dritschel, D. G. 1988 Nonlinear stability bounds for inviscid, two-dimensional, parallel or circular flows with monotonic vorticity, and the analogous three-dimensional quasi-geostrophic flows. *J. Fluid Mech.* **191**, 575–582.

Flierl, G. R. 1988 On the instability of geostrophic vortices. *J. Fluid Mech.* **197**, 349–388.

Helfrich, K. R. & Send, U. 1988 Finite-amplitude evolution of two-layer geostrophic vortices. *J. Fluid Mech.* **197**, 331–348.

Ikeda, M. 1981 Instability and splitting of mesoscale rings using a two-layer quasi-geostrophic model on an f-plane. *J. Phys. Oceanogr.* **11**, 987–998.

Katsman, C. A., Van der Vaart, P. C. F., Dijkstra, H. A. & de Ruijter, W. P. M. 2003 On the stability of multi-layer ocean vortices: a parameter study including realistic Gulf Stream and Agulhas rings. *J. Phys. Oceanogr.* **33**, 1197–1218.

Killworth, P. D., Blundell, J. R. & Dewar, W. K. 1997 Primitive equation instability of wide oceanic rings. Part 1: linear theory. *J. Phys. Oceanogr.* **27**, 941–962.

Lai, D. Y. & Richardson, P. L. 1977 Distribution and movement of Gulf Stream rings. *J. Phys. Oceanogr.* **7**, 670–683.

Olson, D. B. 1991 Rings in the ocean. *Annu. Rev. Earth Planet. Sci.* **19**, 283–311 (referred to herein as O91).

Paldor, N. 1999 Linear instability of barotropic submesoscale coherent vortices observed in the ocean. *J. Phys. Oceanogr.* **25**, 1442–1452.

Paldor, N. & Nof, D. 1990 Linear instability of an anticyclonic vortex in a two-layer ocean. *J. Geophys. Res.* **95**, 18075–18079.

Ripa, P. 1992 Instability of a solid-body rotating vortex in a two-layer model. *J. Fluid Mech.* **242**, 395–417.